Drug Design, Development and Therapy

Dovepress
open access to scientific and medical research

Open Access Full Text Article

ORIGINAL RESEARCH

Involvement of Huanglian Jiedu Decoction on Microglia with Abnormal Sphingolipid Metabolism in Alzheimer's Disease

Yi-Yu Qi[1,*], Xia Heng[1,*], Zeng-Ying Yao[2], Shu-Yue Qu[1], Ping-Yuan Ge[1], Xin Zhao[1], Sai-jia Ni[2], Rui Guo[3], Nian-Yun Yang[1], Qi-Chun Zhang[2], Hua-Xu Zhu[1]

[1]Department of Traditional Chinese Medicine Processing and Preparation, Nanjing University of Chinese Medicine, Nanjing, Jiangsu, People's Republic of China; [2]Department of Pharmacology, Nanjing University of Chinese Medicine, Nanjing, Jiangsu, People's Republic of China; [3]Department of Physiological, Nanjing University of Chinese Medicine, Nanjing, Jiangsu, People's Republic of China

*These authors contributed equally to this work

Correspondence: Qi-Chun Zhang; Hua-Xu Zhu, Email zhangqichun@njucm.edu.cn; zhuhx@njucm.edu.cn

Background: Abnormal sphingolipid metabolism is closely related to the occurrence and development of Alzheimer's disease (AD). With heat-clearing and detoxifying effects, Huanglian Jiedu decoction (HLJDD) has been used to treat dementia and improve learning and memory impairments.

Purpose: To study the therapeutic effect of HLJDD on AD as it relates to sphingolipid metabolism.

Methods: The level of sphingolipids in the brains of APP/PS1 mice and in the supernatant of β-amyloid $(A\beta)_{25-35}$-induced BV2 microglia was detected by HPLC-QTOF-MS and HPLC-QTRAP-MS techniques, respectively. The co-expression of ionized calcium-binding adapter molecule 1 (Iba1) and Aβ as well as four enzymes related to sphingolipid metabolism, including serine palmitoyltransferase 2 (SPTLC2), cer synthase 2 (CERS2), sphingomyelin phosphodiesterase 1 (SMPD1), and sphingomyelin synthase 1 (SGMS1), in the brains of APP/PS1 mice were evaluated by immunofluorescence double labelling. In addition, real-time quantitative reverse transcription-polymerase chain reaction was conducted to determine the mRNA expression of SPTLC2, CERS2, SMPD1, SGMS1, galactosylceramidase (GALC), and sphingosine kinase 2 (SPHK2) in $A\beta_{25-35}$-stimulated BV2 microglia.

Results: Abnormal sphingolipid metabolism was observed both in APP/PS1 mouse brain tissues and $A\beta_{25-35}$-stimulated BV2 cells. The levels of sphingosine, sphinganine, sphingosine-1-phosphate, sphinganine-1-phosphate and sphingomyelin were significantly reduced, while the levels of ceramide-1-phosphate, ceramide, lactosylceramide and hexosylceramide significantly increased in $A\beta_{25-35}$-stimulated BV2 cells. In AD mice, more microglia were clustered in the Aβ-positive region. The decreased level of SGMS1 and increased levels of CERS2, SPTLC and SMPD1 were also found. In addition, the expressions of SPTLC2, CERS2, and SMPD1 in $A\beta_{25-35}$-stimulated BV2 cells were increased significantly, while the expressions of GALC, SPHK2, and SGMS1 were decreased. These changes all showed a significant correction after HLJDD treatment.

Conclusion: HLJDD is a good candidate for treating AD. This study provides a novel perspective on the potential roles of the sphingolipid metabolism in AD.

Keywords: Huanglian Jiedu decoction, HLJDD, Alzheimer's disease, AD, sphingolipid metabolism, HPLC-QTOF-MS, HPLC-QTRAP-MS

Introduction

Alzheimer's disease (AD) is a primary degenerative disease of the central nervous system that occurs in elderly people[1] and has become a major public health problem. Although countless investments have been made in the war against AD, there is currently no known way to prevent or cure this disease. Most of anti-AD drugs have a single molecular target and are mainly acetylcholinesterase inhibitors, which is not an optimal choice for AD patients with multi-pathogenesis.[2]

Received: 5 January 2022
Accepted: 13 March 2022
Published: 30 March 2022

Graphical Abstract

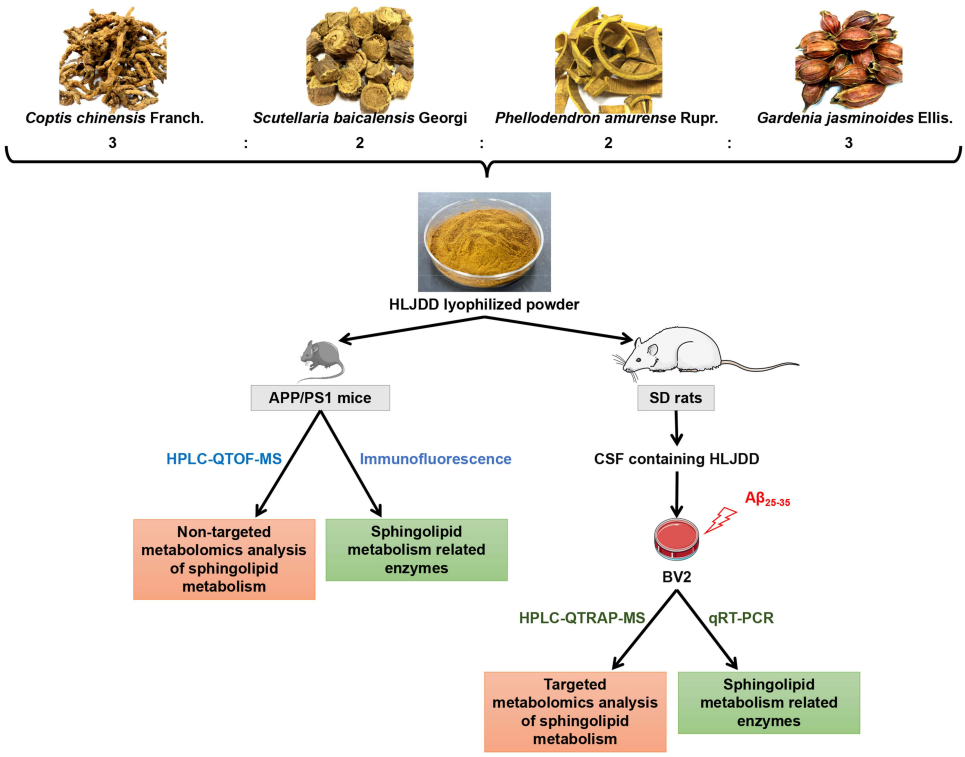

Lipid metabolism is closely related to the production, metabolism and aggregation of Aβ, an important pathological product of AD.[3] Abnormal sphingolipid metabolism occurs in the urine,[4] plasma,[5] brain tissue[6,7] and cerebrospinal fluid[8,9] of AD patients. Sphingolipids are an important class of lipids on cell membranes, mainly including sphingosine (So), sphinganine (Sa), sphingosine-1-phosphate (S1P), sphinganine-1-phosphate (Sa1P), ceramide (Cer), ceramide-1-phosphate (C1P), lactosylceramide (LacCer), hexosylceramide (HexCer) and sphingomyelin (SM). There is a certain correlation between sphingolipid metabolites and the phenotype and function of microglia. A transwell experiments, up-regulation of exosome secretion from neuronal cells by treatment with sphingomyelin synthase 2 (SGMS2) siRNA enhanced Aβ uptake into microglial cells and significantly decreased extracellular levels of Aβ.[10] The key enzyme of the sphingosine metabolism pathway, sphingosine kinase 1 (SPHK1) and its receptor, are expressed in mouse BV2 microglia, and SPHK1 can change the expression and production of pro-inflammatory cytokines and nitric oxide in microglia treated with LPS.[11] Therefore, the regulation of microglial function by sphingolipid metabolites would be a useful and promising approach in the treatment of AD.

The "toxin damaging brain collaterals" theory by Yong-Yan Wang has been brought out[12] and guiding the clinical diagnosis and treatment of brain diseases for decades. This theory refers to the accumulation of toxic, which damages the structure of the brain such as the tiny blood vessels, nerves and brain marrow, and affects the normal physiological function of the brain. In the case of AD, the "brain collaterals" in this theory is equivalent to the "blood brain barrier (BBR) and its carrier function" in modern medicine, and Aβ pertains to "toxicity". The pathogenesis of AD can be described as the accumulation of Aβ may impair the BBR and its carrier function in the brain, which in turn may promote the accumulation of Aβ in the brain.[13] Under the guidance of this theory, the method of detoxification was put forward,[12] such as the use of heat-clearing and detoxification drugs.[14–18] Heat-clearing is to ameliorate the interior pattern or syndromes of exuberant heat, and detoxicating indicates the measure of reducing the virulence and neutralizing the toxicity of pathogens.[19]

Huanglian Jiedu decoction (HLJDD), a representative prescription for heat-clearing and detoxicating, is composed of four herbs: *Coptis chinensis* Franch. (rhizome), *Scutellaria baicalensis* Georgi (radix), *Phellodendron amurense* Rupr. (cortex), and *Gardenia jasminoides* Ellis. (fructus), with a ratio of 3:2:2:3. For centuries, HLJDD has been widely used for the treatment of cerebrovascular diseases, ischaemic stroke, and AD.[20–23] The main active components of HLJDD, alkaloids, flavonoids and iridoids improved the central inflammatory status of AD rats by regulating the levels of inflammatory factors.[24] In addition, HLJDD suppressed gut dysbiosis and the associated Aβ accumulation, controlled neuro-inflammation and reversed cognitive impairment.[2] In our previous study,[25] HLJDD-treated APP/PS1 mice showed better performance than vehicle-treated APP/PS1 mice in the Morris water maze test. Meanwhile, in the spatial exploration test, the crossing platform frequency of HLJDD mice was significantly higher than that of model mice. Regulation of microglial activation by HLJDD has also been observed, suggesting that HLJDD inhibits central nervous system inflammation in APP/PS1 mice. The results of blood non-targeted metabolomics suggested that the adjustment of sphingolipid metabolism was accompanied by improved learning and memory in HLJDD-treated APP/PS1 mice. Therefore, we speculate that the therapeutic effect of HLJDD on APP/PS1 mice may be related to microglial sphingolipid metabolism.

At present, few studies have explored the mechanism of HLJDD in the treatment of AD from the perspective of sphingolipid metabolism. Hence, we firstly performed HPLC-QTOF-MS combined with HPLC-QTRAP-MS techniques to determine whether HLJDD improves AD by relating sphingolipids level in vivo and in vitro. Then, immunofluorescence double labelling and real-time quantitative reverse transcription-polymerase chain reaction (qRT-PCR) were conducted to determine the expression of sphingolipid metabolizing enzymes. Our study provides a new idea for the mechanism of HLJDD treatment of AD.

Materials and Methods

Herbal Medicine and Reagents

Coptis chinensis Franch. (rhizome) (batch number, 1711028050), *Scutellaria baicalensis* Georgi (radix) (batch number, 1709019024), *Phellodendron amurense* Rupr. (cortex) (batch number, 1709016005), and *Gardenia jasminoides* Ellis. (fructus) (batch number, 1711018022) were purchased from Anhui Huizhongzhou Traditional Chinese Medicine Pieces Co., Ltd. (Anhui, China) and authenticated by Dr. Qinan Wu (Professor of Pharmacognosy, College of Pharmacy, Nanjing University of Chinese Medicine, Nanjing, China). Voucher specimens were deposited at Nanjing University of Chinese Medicine. A LIPID MAPS internal standard cocktail (internal standards mixture II, 25 μM in ethanol, catalogue LM-6005) was purchased from Avanti Polar Lipids (Alabaster, USA). Aβ peptide (25–35) ($A\beta_{25\text{-}35}$) was obtained from Beijing Bosen Biotechnology Co., Ltd. (Beijing, China). TRIzol total RNA extraction reagent and BeyoRT™ II first strand cDNA synthesis kit were purchased from Biyuntian Biotechnology Co., Ltd. (Shanghai, China). TB Green® Premix Ex Taq™ II was purchased from Baori Biotechnology Co., Ltd. (Beijing, China).

The following primary antibodies were used in these experiments: rabbit anti-CERS2 (Abcam, ab176709, 1:200), rabbit anti-SPTLC2 (Proteintech, 51012-2-AP, 1:200), rabbit anti-SGMS1 (Proteintech, 19050-1-AP, 1:50), rabbit anti-SMPD1 (Proteintech, 14609-1-AP, 1:200), rabbit anti-Aβ polyclonal (Proteintech, 25524-1-AP, 1:200), and goat anti-Iba-1 (Abcam, ab48004, 1:50). Secondary antibodies for the immunofluorescence study were donkey anti-goat IgG H&L (Alexa Fluor® 488) (Abcam, ab150129) and donkey anti-rabbit IgG H&L (Alexa Fluor® 555) (Abcam, ab150074).

Preparation of the Huanglian Jiedu Decoction Extract

HLJDD solution was extracted according to the preferred extraction protocol used in our laboratory.[26] Analysis of the constituents of HLJDD was carried out using HPLC with berberine, baicalin and geniposide as standards (Agilent 1260, USA). For reagents and experimental procedures, see the "Determination of the main pharmacodynamic components of HLJDD" section in the Supplementary Materials. The abundances of berberine, baicalin, and geniposide in the freeze-

dried powder of HLJDD were 7.67%, 11.46%, and 2.42%, respectively (Figure S1, Table S1). The powder was dissolved in 0.5% carboxymethyl cellulose sodium salt (CMC-Na) solution for use.

Non-Targeted Metabolomics Analysis of Sphingolipid Metabolism in APP/PS1 Mouse Brain Tissue

Animals and Drug Treatment

SPF male APP/PS1 (B6C3-Tg (APPswe, PSEN1dE9) 85Dbo/MmJ) double transgenic mice (21 weeks), weighing 27.92 ±2.00 g, were purchased from the Experimental Animal Center of the Fourth Military Medical University of the People's Liberation Army and used as the AD model. SPF male C57BL/6 mice (21 weeks), weighing 28.00±2.00 g, were used as blank controls (wild type, WT). The mice were adaptively reared for a week in an environment controlled by light (12/12 h day and night cycle), temperature (25±1°C) and humidity (60±5%) and were randomly divided into 3 groups with 10 mice each: WT group, APP/PS1 group and APP/PS1-HLJDD group (treated with HLJDD at 2.28 g/kg). The HLJDD dosage was calculated using the dosage conversion relationship between mice and humans and the clinical dosage of the HLJDD extract. At the age of 22 weeks, the mice were continuously treated by intragastric administration for 9 weeks. Mice in the WT and APP/PS1 groups were given 0.5% CMC-Na. HLJDD and 0.5% CMC-Na were administered at 0.2 mL/10 g body weight. The study was performed following recommendations provided by the Guide for the Care and Use of Laboratory Animals of the National Institutes of Health (NIH Publication No. 80–23; revised 1978). The Animal Care and Use Committee of Nanjing University of Chinese Medicine approved the protocol and the total number of mice used in this study (No. 202010A022, Item No. 012071001462).

Brain Sample Collection and Processing

After 9 weeks of treatment, 6 mice were randomly selected from each group, brain samples were collected and weighed immediately, and the samples were stored at −80°C until analysis. Brain samples were homogenized by adding 10 volumes of double distilled water. One hundred microlitres of homogenized solution was used to extract the sphingolipid components according to Wang's[27] improved method. The extract was evaporated to dryness in vacuo using a Labconco CentriVap concentrator (Kansas City, USA), and the residues were reconstituted with 100 μL of methanol and vortexed for 120 s. After centrifugation at 14,000 rpm for 10 min at 4°C, the supernatant was transferred to an autosampler vial for further HPLC-QTOF/MS analysis. Five microlitres of brain sample homogenate solution from each group was pooled as quality control (QC) samples and processed according to the above method to obtain quality control samples. During the whole analysis process, QC samples were run every 6 samples to monitor the reproducibility and stability of the LC-MS system throughout the whole operation process.

Liquid Chromatography and Mass Spectrometry

Chromatographic experiments were performed on a Shimadzu LC-20A Series HPLC system (Shimadzu, Japan). A 2 μL aliquot of sample solution was injected into a Poroshell 120 EC-C18 column (2.1 mm × 100 mm, 2.7 μm) maintained at 40°C, and the flow rate was 0.4 mL/min. The mobile phase consisted of solvent A (methanol: H_2O: formic acid = 60: 40: 0.2, *v/v/v*, 10 mM ammonium acetate) and solvent B (methanol: isopropyl alcohol: formic acid = 60: 40: 0.2, *v/v/v*, 10 mM ammonium acetate). The column was eluted with a gradient of 0 to 10% B at 0–3 min; 10% to 40% B at 3–5 min; 40% to 55% B at 5–5.3 min; 55% to 60% B at 5.3–8 min; 60% to 80% B at 8–8.5 min; 80% B at 8.5–10.5 min; 80% to 90% B at 10.5–16 min; 90% B at 16–19 min; 90% to 100% B at 19–22 min, followed by washing with 100% B and equilibration with 0% B. A typical run time was 20 min.

Mass spectrometry was performed on an AB SCIEX Triple TOF^{TM} 5600 system (AB SCIEX, USA). Nitrogen was used as the atomizing gas and cone gas. The electrospray ion (ESI) source adopted the positive ion scanning mode, and the mass scanning range was 50–1500 *m/z*. The conditions used for the ESI source were as follows: ion spray voltage of 5.5 kV, electrospray ionization temperature of 550°C, nebulizer gas of 55 psi, drying gas of 55 psi, curtain gas of 35 psi, and decluttering potential of 100 V. Data were collected by the Analyst TF system (version 1.6, AB SCIEX) and analyzed by Peak View software (version 2.0, AB SCIEX).

Data Extraction and Preprocessing

The raw data collected by mass spectrometry were initially processed by AB SCIEX's Marker View 1.2.1 software. The specific operation flow and parameter settings are as follows: 1) Data reading: wiff format maps were imported into the Marker View software; 2) Chromatographic peak identification: retention time was set to 0–22 min, minimum peak width was set to 25 ppm, minimum retention time peak width was set to 6 scans, and noise threshold was set to 100; 3) Peak alignment: retention time deviation tolerance was set to 0.1 min; 4) Peak filtration: the peaks that did not appear in 80% of the samples were removed, the threshold for extracting the number of peaks was set to 8000; and 5) Normalization: the data were normalized using the total peak area normalization method.

Qualitative Analysis of Sphingolipids and Multivariate Statistical Analysis

The LIPID MAPS (http://www.lipidmaps.org/) database was searched, the literature was consulted, as many sphingolipid components were selected as possible, and the related molecular formulas, names, structures and classifications were organized to establish the target compound list. Then, PeakView software was used to import original maps, and the primary chromatographic information was extracted through XIC Manager. Qualitative analyses of sphingolipids were performed based on secondary fragmentation information and the cleavage pattern of differently classified SPLs in the literature and database.

Based on the extracted and preprocessed data, the peak areas of the identified sphingolipid components in different groups were extracted and imported into SIMCA 14.1 software for multivariate statistical analysis. Variables with VIP values greater than 1 in orthogonal projection to latent structures discriminant analysis (OPLS-DA) and P values less than 0.05 in the Mann–Whitney *U*-test were considered to be statistically significant. Then, the variation trend of these variables in each group was analyzed.

Targeted Metabonomic Analysis of Sphingolipid Metabolism in $A\beta_{(25-35)}$ Oligomer-Stimulated BV2 Microglia

Collection of Cerebrospinal Fluid (CSF) Containing HLJDD

SPF male SD rats (7 weeks), weighing 260–280 g (Animal Multiplication Center of Qigong Mountain, Nanjing, China) were housed in an animal laboratory with regulated temperature and humidity of 25±1°C and 60±5%, respectively. Animals were acclimatized for one week and randomly divided into 2 groups with 25 rats each: the control group and HLJDD group (treated with HLJDD at 1.58 g/kg/day). The animals were continuously treated for one week. Rats in the control group were given 0.5% CMC-Na. HLJDD and 0.5% CMC-Na were given by intragastric administration at 0.2 mL/10 g of body weight. The HLJDD dosage was calculated using the dosage conversion relationship between rats and humans and the clinical dosage of the HLJDD extract. After one week of treatment, the CSF of the two groups of rats was collected by the occipital macroscopic puncture method and stored at −80°C until use. The study was carried out following recommendations provided by the Guide for the Care and Use of Laboratory Animals of the National Institutes of Health (NIH Publication No. 80-23; revised 1978). The Animal Care and Use Committee of Nanjing University of Chinese Medicine approved the protocol and the total number of rats used in this study (No. 202011A008, Item No. 012071001462).

CSF samples containing HLJDD have been detected in our previous study.[28] Nine active compounds (berberine, berberrubine, jatrorrhizine, palmatine, baicalin, wogonin, oroxylin A, geniposide and gardenin B) could enter the brain tissue through the blood-brain barrier and distribute in CSF. Among them, geniposide (58.16±4.38 ng/mL) was the highest content, followed by berberine (41.07±3.61 ng/mL) and berberrubine (37.44±0.28 ng/mL).

Preparation of $A\beta_{25-35}$ Oligomers

$A\beta_{25-35}$ was dissolved in sterile distilled water to obtain an $A\beta_{25-35}$ solution with a concentration of 1 mM, which was then incubated at 37°C for 72 h.[29] The $A\beta_{25-35}$ oligomers were stored at −20°C for later use.

Cell Culture, Treatment and Morphological Analysis

BV2 microglia were purchased from the China Center for Type Culture Collection (Hubei, China) and cultured in DMEM containing 10% FBS, 100 U/mL of penicillin and 100 μg/mL of streptomycin at 37°C in a humidified incubator with 5% CO_2. BV2 microglia were pretreated with 5% CSF containing HLJDD (Aβ-HLJDD group) or CSF from control rats (Aβ group) 1 h, followed by incubation with $A\beta_{25\text{-}35}$ oligomer (20 μM) for 24 h. For morphological analysis, cells were imaged with the inverted microscope (TS2-S-SM, Nikon, Japan) at 200× magnification.

Extraction of Sphingolipid Components in Cell Culture Supernatants

A total of 500 μL cell culture supernatant was placed in a freeze dryer for drying. These samples were processed according to Wang's[27] improved method for extraction of sphingolipid components and brain tissue samples. The extracts were evaporated to dryness in vacuo using a Labconco CentriVap concentrator, and the residues were reconstituted with 250 μL of methanol and vortexed for 120 s. After centrifugation at 14,000 rpm for 10 min at 4°C, the supernatant was transferred to an autosampler vial for further HPLC-QTRAP-MS analysis.

Liquid Chromatography and Mass Spectrometry

Chromatographic experiments were performed on a Shimadzu LC-20A Series HPLC system (Shimadzu, Japan). Each aliquot of the samples and standard solution (4 μL) was injected into a Poroshell 120 EC-C18 column (2.1 mm × 100 mm, 2.7 μm) maintained at 40°C, and the flow rate was 0.3 mL/min. The mobile phase and gradient elution procedures were identical to those previously described for HPLC-QTOF/MS.

Mass spectrometry was performed on an AB SCIEX Triple Quad™ 5500 linear ion hydrazine mass spectrometer (AB SCIEX, USA) using an ESI source operated in positive mode. The main parameters were set as follows: ion source temperature 550°C, spray voltage 5500 V, curtain gas 241.32 kPa, atomization gas 379.22 kPa, and dry gas 379.22 kPa. The analytes were determined by multiple reactions monitoring mode. The full scan, selective ion scan, and product ion scan modes were used to determine the mass spectrometry parameters of each compound. Data were collected and analyzed by Analyst software (version 1.6, AB SCIEX). The content of each compound under different treatments was calculated by the integrated peak area.

Analysis of Enzymes Related to Sphingolipid Metabolism

Double Immunofluorescence Labelling

Four mice from the WT, APP/PS1 and APP/PS1-HLJDD groups were underwent transcardiac perfusion with saline and then 4% PFA. The brain samples were taken out rapidly and embedded in paraffin blocks using a paraffin embedding station (Leica Biosystems Nussloch GmbH, Leica EG1150H, Germany), and then sectionalized (5 μm) using a rotary microtome (Leica Biosystems Nussloch GmbH, Leica RM2245, Germany). Sections were immersed in xylol for 10 min 3 times and rehydrated in a series of graded alcohol solutions (absolute ethyl alcohol was diluted to 90%, 80%, and 70%) for 5 min each. Antigen retrieval was achieved by dipping the sections in hot citrate buffer (10 mM, pH 6.0) and heating the sections in an autoclave for 8 min. As the sections cooled to room temperature, the sections were rinsed with water and immersed in 3% H_2O_2 for 10 min to abolish endogenous peroxidase activity. Brain sections from each mouse group were incubated with the following primary antibodies: rabbit anti-CERS2, rabbit anti-SPTLC2, rabbit anti-SGMS1, rabbit anti-SMPD1, rabbit anti-Aβ polyclonal, and goat anti-Iba1 at 4°C overnight. After thorough washing, sections were then incubated for 1 h at room temperature with donkey anti-goat IgG H&L (Alexa Fluor® 488) or donkey anti-rabbit lgG H&L (Alexa Fluor® 555) and then processed with DAPI for 10 min. Five to ten brain sections from individual mice were assessed for each antibody. ImageJ 1.53c was used to calculate the mean integrated density in CA3 region.

Real-Time Quantitative Reverse Transcription-Polymerase Chain Reaction (qRT-PCR)

Total RNA was isolated with TRIzol total RNA extraction reagent according to the manufacturer instructions. NanoDrop One C (Thermo Fisher™, USA) was employed to determine the concentration of RNA. A BeyoRT™ II first strand

Table 1 Information of Primer Sequence

Primer	Forward	Reverse
SPTLC2	5′AACGGGGAAGTGAGGAACG3′	5′CAGCATGGGTGTTTCTTCAAAAG3′
CERS2	5′ATGCTCCAGACCTTGTATGACT3′	5′CTGAGGCTTTGGCATAGACAC3′
GALC	5′CGCCTACGTGCTAGACGAC3′	5′ACGATAGGGCTCTGGGTAATTT3′
SPHK2	5′CACGGCGAGTTTGGTTCCTA3′	5′CTTCTGGCTTTGGGCGTAGT3′
SMPD1	5′TGGGACTCCTTTGGATGGG3′	5′CGGCGCTATGGCACTGAAT3′
SGMS1	5′GAAGGAAGTGGTTTACTGGTCAC3′	5′GACTCGGTACAGTGGGGGT3′
GAPDH	5′AGGTCGGTGTGAACGGATTTG3′	5′TGTAGACCATGTAGTTGAGGTCA3′

cDNA synthesis kit was used to reverse transcribe RNA (0.2–1.0 μg) in a 20-μL reaction volume (42°C, 30 min; 95°C, 5 min); then, cDNA (2 μL) was amplified using TB Green® Premix Ex Taq™ II. All tests were performed in duplicate 20 μL reaction mixtures in 96-well plates, and a negative control without cDNA template was included in each run. Visual inspection of the melting curves was used to confirm the specificity of the products during PCR. The expression level of a gene was calculated using the $2^{-\Delta\Delta Ct}$ method[30] with glyceraldehyde-3-phosphate dehydrogenase (GAPDH) as the internal control. The primer sequences of serine palmitoyltransferase 2 (SPTLC2), cer synthase 2 (CERS2), galactosylceramidase (GALC), sphingosine kinase 2 (SPHK2), sphingomyelin phosphodiesterase 1 (SMPD1), sphingomyelin synthase 1 (SGMS1) and GAPDH were obtained from primerbank database (https://pga.mgh.harvard.edu/primerbank/), and were described in Table 1. The qRT-PCR amplification reaction conditions were as follows: predenaturation at 95°C for 30s, 40 cycles of denaturation at 95°C for 10s, and annealing at 53°C for 60s.

Statistical Analysis

All data were statistically analyzed using GraphPad prism 6.0 (GraphPad Software). The significance of differences was assessed by one-way analysis of variance (ANOVA) followed by Tukey's post hoc multiple comparisons test. Data were expressed as the mean±SD. Differences were considered to be significant when $p<0.05$ or $p<0.01$.

Results

Non-Targeted Metabolomics Analysis of Sphingolipid Metabolism in the Brains of APP/PS1 Mice

The overlapping total ion chromatogram of QC samples in the ESI+ scan mode showed repeatability and stability of HPLC-QTOF/MS analytical methods (Figure 1A). Cer is the simplest sphingolipid composed of sphingosine and a molecule of fatty acid. Galactose/glucose forms a cerebroside at the C-1 position of Cer via a β-glycosidic bond. Since the long-chain base structure contained in Cer and cerebroside in mammals is mainly d18:1, a long-chain base with an *m/z* of 264 is easily produced; if a dihydrosphingosine backbone is present, an ion fragment with an *m/z* of 266 is produced; phosphorylcholine or phosphoethanolamine is substituted for the Cer terminal hydroxyl group to form a sphingomyelin, resulting in a choline ion fragment with an *m/z* of 184.[27,31] According to the structure and cleavage rule of sphingolipids (Figure 1B), 45 sphingolipids were identified, including So, Sa, Cer, dihydroceramide, cerebroside, sulfatide and SM (Figure 1C).

Compared with WT mice, APP/PS1 mice showed significant changes in sphingolipid metabolism (Figure 1D). To further analyze the effect of AD disease status on sphingolipid metabolism, variables with a VIP>1 in OPLS-DA and a P<0.05 in the Mann–Whitney *U*-test were selected, and these variables were considered to have significant changes in the disease state. A total of 17 metabolites contributed to the grouping (Table 2); among them, 9 sphingolipid metabolites, especially Cer, were adjusted back to normal levels after HLJDD intervention (Figure 1E). These results suggested that Cer may be a critical target for AD therapy.

Effects of HLJDD on Microglial Activation

To investigate the effects of HLJDD on the activation of BV2 cells stimulated by $A\beta_{25-35}$, the morphological changes in BV2 cells were evaluated. As indicated in Figure S2A, resting microglia were spindle-shaped with small cell

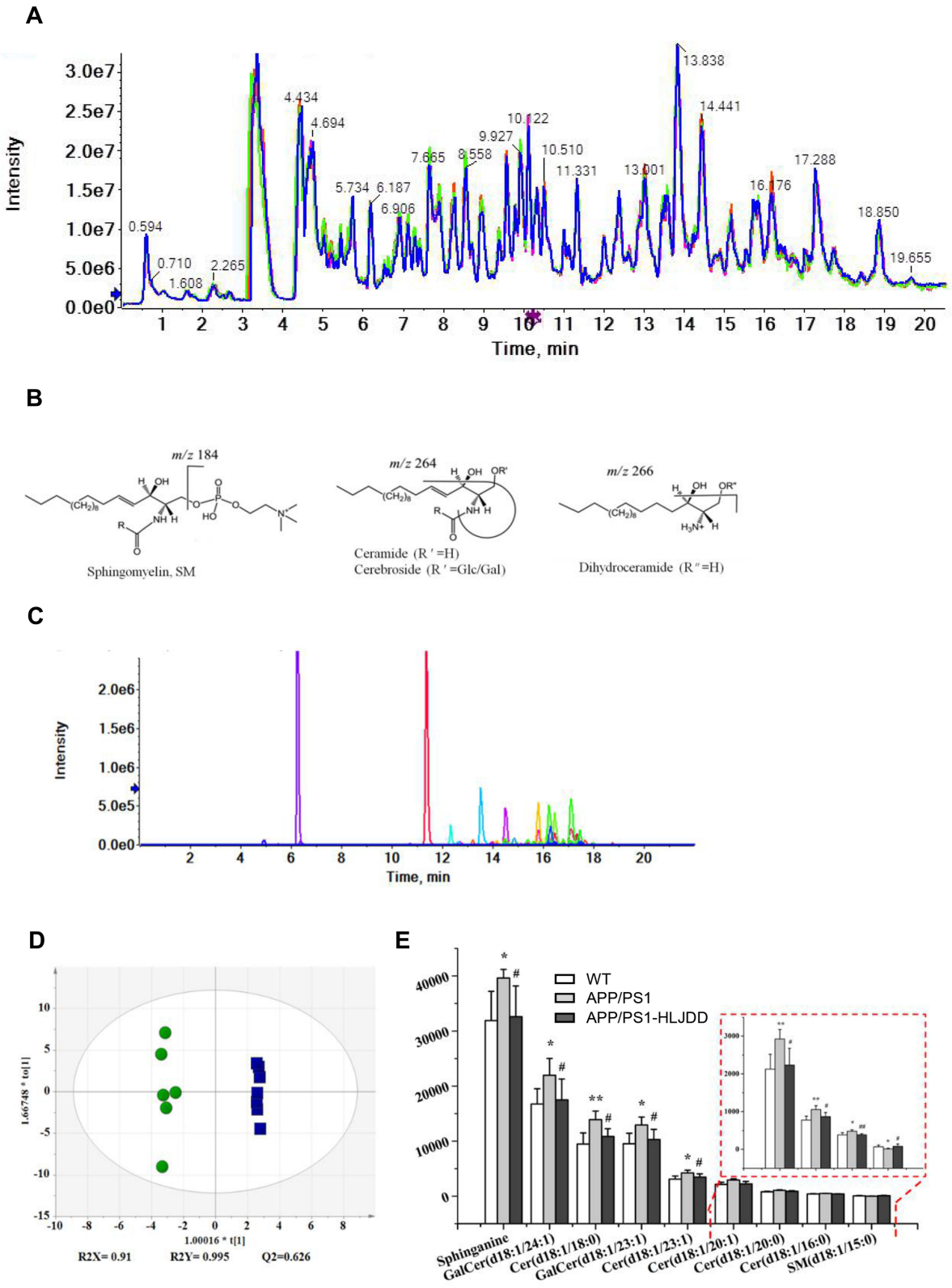

Figure 1 Change in sphingolipid metabolism in brain tissues of AD mice and the effects of HLJDD treatment. (**A**) Overlapping total ion chromatogram of QC samples in positive ion mode. (**B**) Common structure and lysis of sphingolipids. (**C**) Primary extraction chromatogram of 45 sphingolipids. (**D**) OPLS-DA score plots comparing WT (green, circle) and APP/PS1 mice (blue, rectangle). (**E**) Sphingolipid components that returned to normal levels after HLJDD intervention. Data are shown as the means ± SD (n ≥ 6, WT vs APP/PS1, $^{*}p < 0.05$, $^{**}p < 0.01$; APP/PS1 vs APP/PS1-HLJDD, $^{\#}p < 0.05$, $^{\#\#}p < 0.01$).

Table 2 Specific Information and Trends of Sphingolipid Metabolites in Non-Targeted Metabolomics Analysis

No.	Metabolite	Formula	RT (min)	Measured *m/z*	Error (ppm)	VIP	Trend
1	C16 So	$C_{16}H_{33}NO_2$	4.92	272.2587	1.2	1.02	↑*
2	Sa	$C_{18}H_{39}NO_2$	6.26	302.3067	4.6	1.34	↑*
3	Cer (d18:1/16:0)	$C_{34}H_{67}NO_3$	13.12	538.5209	2.8	1.09	↑*
4	Cer (d18:1/18:0)	$C_{36}H_{71}NO_3$	14.51	566.5512	1.0	1.68	↑**
5	Cer (d18:1/20:1)	$C_{38}H_{73}NO_3$	14.42	592.5640	−3.9	1.50	↑**
6	Cer (d18:1/20:0)	$C_{38}H_{75}NO_3$	12.70	594.5820	0.0	1.11	↑**
7	Cer (d18:1/22:1)	$C_{40}H_{77}NO_3$	15.74	620.5971	−0.9	1.16	↑*
8	Cer (d18:1/22:0)	$C_{40}H_{79}NO_3$	17.16	622.6152	3.2	1.24	↑**
9	Cer (d18:1/23:1)	$C_{41}H_{79}NO_3$	16.39	634.6155	3.5	1.58	↑*
10	Cer (d18:1/24:1)	$C_{42}H_{81}NO_3$	17.15	648.6285	−0.7	1.36	↑*
11	GalCer (d18:1/20:1)	$C_{44}H_{83}NO_8$	14.47	754.6193	0.2	1.23	↑*
12	GalCer (d18:1/22:1)	$C_{46}H_{87}NO_8$	15.73	782.6535	3.9	1.23	↑*
13	GalCer (d18:1/23:1)	$C_{47}H_{89}NO_8$	16.46	796.6669	1.0	1.54	↑*
14	GalCer (d18:1/24:1)	$C_{48}H_{91}NO_8$	17.11	810.6815	−0.3	1.47	↑*
15	SM (d18:1/15:0)	$C_{38}H_{77}N_2O_6P$	11.72	689.5595	0.4	1.02	↓*
16	SM (d18:1/18:0)	$C_{41}H_{83}N_2O_6P$	13.53	731.6062	0.8	1.21	↑*
17	SM (d18:0/22:0)	$C_{45}H_{93}N_2O_6P$	16.72	789.6844	−0.6	1.04	↓*

Notes: (↑/↓indicates higher/lower content, respectively, in the APP/PS1 group compared with the WT group; *$p < 0.05$, **$p < 0.01$).

bodies and long processes. However, $A\beta_{25-35}$-stimulated BV2 cells presented a typical activated state, which was characterized by cell body enlargement and retracted processes (Figure S2B). These phenomena were attenuated after HLJDD treatment (Figure S2C). The results suggest that HLJDD could reverse the morphological changes induced by $A\beta_{25-35}$.

Targeted Metabolomics Analysis of Sphingolipid Metabolism in Microglia

The structure of sphingolipids has a very complex molecular composition due to the difference in the length of the fatty acid carbon chain, the number of double bonds, and the number of hydroxyl groups. When sufficient standards cannot be obtained, it is not possible to accurately determine the species of sphingolipids based on precursor ions and characteristic product ion fragments. However, the retention time of sphingolipids species varies with the different molecular weight due to the various length of the carbon chain, the number of double bonds, and the number of hydroxyl groups. Specifically, when the carbon chain of the sphingolipid molecule species is shorter, the double bond and the hydroxyl group are more obvious, the retention time is shorter, and the longer is reverse. The carbon chain length and retention time of the same sphingolipid molecule species with the same double bond and hydroxyl group show a certain degree index relationship.[32] Therefore, after inferring the structure from the precursor ion and characteristic product ion fragments, we verified the accuracy by combining the relationship between retention time and structure. The exponential relationship between carbon chain length and retention time was shown in Figure 2A–D. When Cer, LacCer, HexCer and SM have the same double bond and hydroxyl number, the carbon chain length and retention time can be fitted to a good exponential equation (R^2>0.99). For the five components (So, Sa, S1P, Sa1P and C1P), the number of these molecules detected was too small, so the numbers were not sufficient to fit the exponential equation, but the retention time of each molecular species of the same sphingolipid component increased with increasing carbon chain length, which also roughly verified its accuracy.

Finally, 49 sphingolipid molecular species were detected (Figure 3A–F, Table S2). Among them, 30 sphingolipid molecular species showed significant changes (Table 3). The total level of 9 types of sphingolipids (Table S3) in each cell culture fluid group was obtained after statistical analysis of the levels of various sphingolipid molecules. The levels of So, Sa, S1P, Sa1P and SM were significantly reduced in the model group, while the levels of C1P, Cer, LacCer and HexCer showed an upward trend after Aβ induction, and these changes returned to normal levels after treatment with CSF containing HLJDD (Figure 4A–I). These results suggested that Cer may be a critical target for AD therapy. These

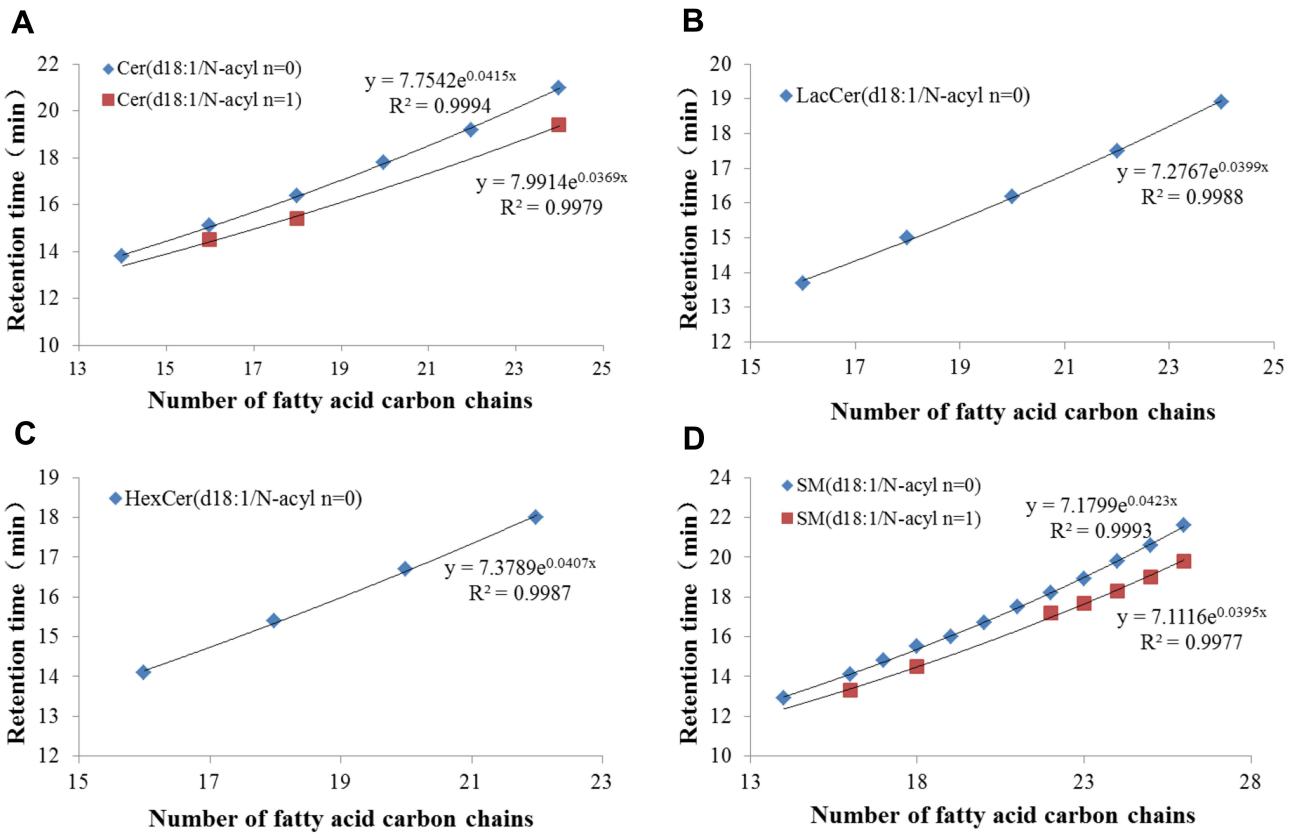

Figure 2 Index equation of fatty acid carbon chain number and retention time of various sphingolipids. Cer (**A**), LacCer (**B**), HexCer (**C**) and SM (**D**). The n means the number of double bonds.

results showed that the disorder of sphingolipids metabolism in AD occurs on microglia, which suggests that reprogramming of sphingolipids metabolism in microglia and intervention of HLJDD may be a direction for the treatment of AD.

Double Immunofluorescence Labelling Analysis of Sphingolipid Metabolizing Enzymes in APP/PS1 Mice

Clearly, in CA3 region of APP/PS1 mice, the plaques immune-stained with Aβ were increased relative to WT group, which is the usual pathology of AD (Figure 5A). Microglia were activated in the AD state, which then induces and maintains a chronic inflammatory state, leading to neuronal damage and neurodegeneration.[33] As shown in Figure 5A, APP/PS1 mice showed significant microglial aggregation in the Aβ immune-staining region. After HLJDD intervention, the activation of microglia around Aβ plaques was reduced (Figure 5A). In order to observe the effect of HLJDD on microglia sphingolipid metabolism under AD condition, we performed immunofluorescence and we found that HLJDD increased the level of SGMS1 and decreased the level of CERS2, SPTLC and SMPD1 (Figure 5B–E). These results suggest that inhibiting the activation of microglial inflammatory phenotypes may be one of the mechanisms by which HLJDD improves AD. More importantly, HLJDD could regulate the metabolism of sphingolipids in microglia under AD pathological conditions.

qRT-PCR Analysis of Sphingolipid Metabolizing Enzymes in Microglia

We also examined the expressions of sphingolipid metabolizing enzymes in $A\beta_{25\text{-}35}$-stimulated BV2 cells. Sphingolipid metabolism-related enzymes were changed significantly after different treatments. The expressions of SPTLC2, CERS2, and SMPD1 in $A\beta_{25\text{-}35}$-stimulated BV2 cells were increased significantly, while the expressions of GALC, SPHK2, and

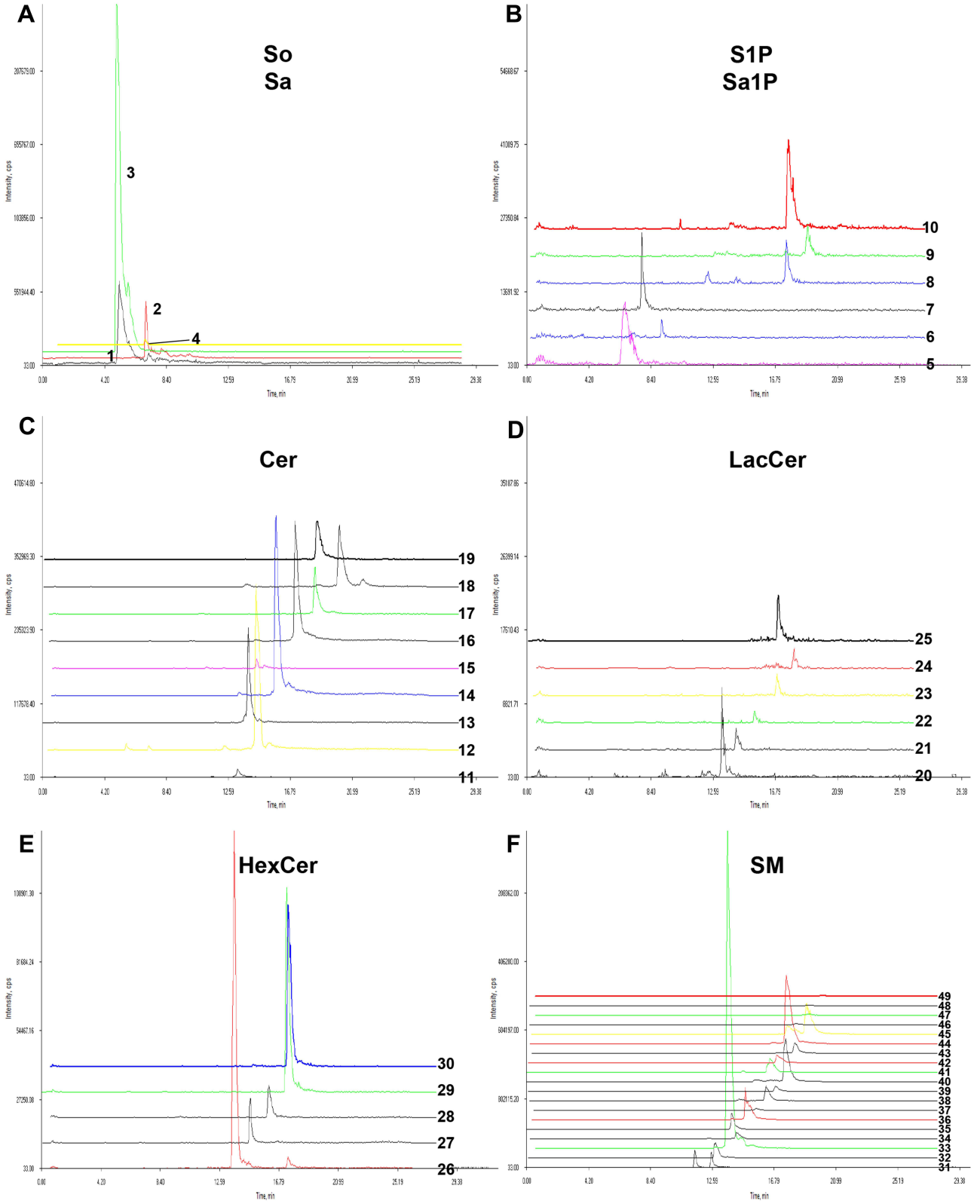

Figure 3 Extracted ion chromatograms of 49 sphingolipid species. (**A**) So and Sa, (**B**) S1P and Sa1P, (**C**) Cer, (**D**) LacCer, (**E**) HexCer and (**F**) SM. Numbers are the same as those in Table S2.

Table 3 Species of Sphingolipids with Significant Changes in Targeted Metabolomics Analysis

No.	Compound	Concentration (nmol/mL Cell Culture Fliud)/(Unexpected Text Node "x")		
		CON	Aβ	Aβ-HLJDD
1	So (d16:1)	351.46±8.02	309.58±13.14**	423.93±38.61##
2	So (d18:1)	106.66±5.54	91.37±3.98**	112.63±5.94##
3	Sa (d16:0)	5098.56±186.85	4360.87±318.85**	7248.34±305.64##
4	Sa (d18:0)	20.76±3.89	9.88±3.95**	18.57±2.59##
5	S1P (d16:1)	10.28±0.77	7.47±0.56**	10.51±2.21##
6	S1P (d19:1)	3.36±0.08	3.10±0.02**	3.56±0.05##
7	Sa1P (d16:0)	5.01±0.27	3.67±0.18**	6.47±0.76##
8	C1P (d18:1/14:0)	1.25±0.21	1.48±0.13*	1.08±0.23##
9	C1P (d18:1/16:0)	0.45±0.32	0.89±0.19*	0.20±0.54#
10	Cer (d18:1/16:0)	240.06±14.00	296.20±11.05**	58.28±7.78##
11	Cer (d18:1/18:0)	56.45±9.20	93.60±14.28**	68.50±10.21##
12	Cer (d18:1/20:0)	6.56±1.30	9.62±0.63**	4.72±0.21##
13	Cer (d18:1/24:0)	22.01±5.50	50.70±14.06**	21.95±3.56##
14	Cer (d18:1/24:1)	18.77±4.78	24.15±1.85*	20.76±0.84##
15	LacCer (d18:1/18:0)	3.55±0.20	3.82±0.15*	3.13±0.23##
16	LacCer (d18:1/20:0)	2.69±0.14	2.86±0.09*	2.74±0.05#
17	LacCer (d18:1/22:0)	4.18±0.22	4.49±0.24*	3.72±0.41##
18	HexCer (d18:1/16:0)	53.88±5.07	65.21±10.18*	45.36±6.06##
19	HexCer (d18:1/18:0)	3.88±0.49	5.18±1.11*	3.26±1.12#
20	HexCer (d18:1/20:0)	3.05±0.47	4.53±1.10*	3.44±0.76#
21	HexCer (d18:1/22:0)	35.72±6.02	44.82±7.54*	31.59±4.73##
22	SM (d18:1/17:0)	14.57±2.08	10.92±1.85**	13.53±2.01#
23	SM (d18:1/18:1)	20.49±1.19	24.86±4.45*	20.04±1.57#
24	SM (d18:1/18:0)	57.42±5.34	47.70±3.26**	53.95±4.69#
25	SM (d18:1/20:0)	26.35±3.55	21.46±2.95*	26.86±4.33#
26	SM (d18:1/22:0)	97.15±7.53	83.64±1.55**	106.27±20.08#
27	SM (d18:1/23:0)	25.18±2.13	22.09±0.87**	23.53±0.80#
28	SM (d18:1/24:0)	88.96±5.33	73.56±3.79**	84.97±3.79##
29	SM (d18:1/25:1)	3.80±0.33	3.35±0.23*	3.77±0.38#
30	SM (d18:1/26:0)	1.51±0.27	1.20±0.12*	1.52±0.08##

Notes: (n=6, CON vs Aβ, *$p < 0.05$, **$p < 0.01$; Aβ vs Aβ-HLJDD, #$p < 0.05$, ##$p < 0.01$).

SGMS1 showed the opposite trend, and these changes all showed a significant correction after treatment with 5% CSF containing HLJDD (Figure 6A–F).

Sphingolipid components and enzymes related to sphingolipid metabolism that significantly changed after $A\beta_{25-35}$ oligomer induction and HLJDD intervention were screened, and their changes in the sphingolipid metabolism pathway were labelled to obtain a schematic diagram of the changes in the sphingolipid metabolism pathway (Figure 7).

Discussion

AD is a common neurodegenerative disease. With the increasing prevalence of AD, the demand for drugs to treat AD has become increasingly urgent. Heat clearing and detoxification, as one of the treatment rules of AD, have shown good application prospects in AD treatment in recent years.[34] HLJDD, a classic prescription in heat-clearing and detoxifying decoctions, was used in China and Japan to treat stroke and dementia.[35,36] A previous experiment[25] by our research group found that HLJDD can improve learning and memory impairments in APP/PS1 mice during the Morris water maze test. In addition, the metabolomics results of APP/PS1 plasma samples indicated that neuro-inflammation and lipid metabolism disorders (including sphingolipid metabolism) may be important pathogenic factors in the pathogenesis of AD. In this study, we mainly used non-targeted metabolomics and targeted metabolomics to analyze the changes in sphingolipid metabolism in the brains of APP/PS1 mice after HLJDD treatment and in $A\beta_{25-35}$-stimulated BV2 microglia treated with

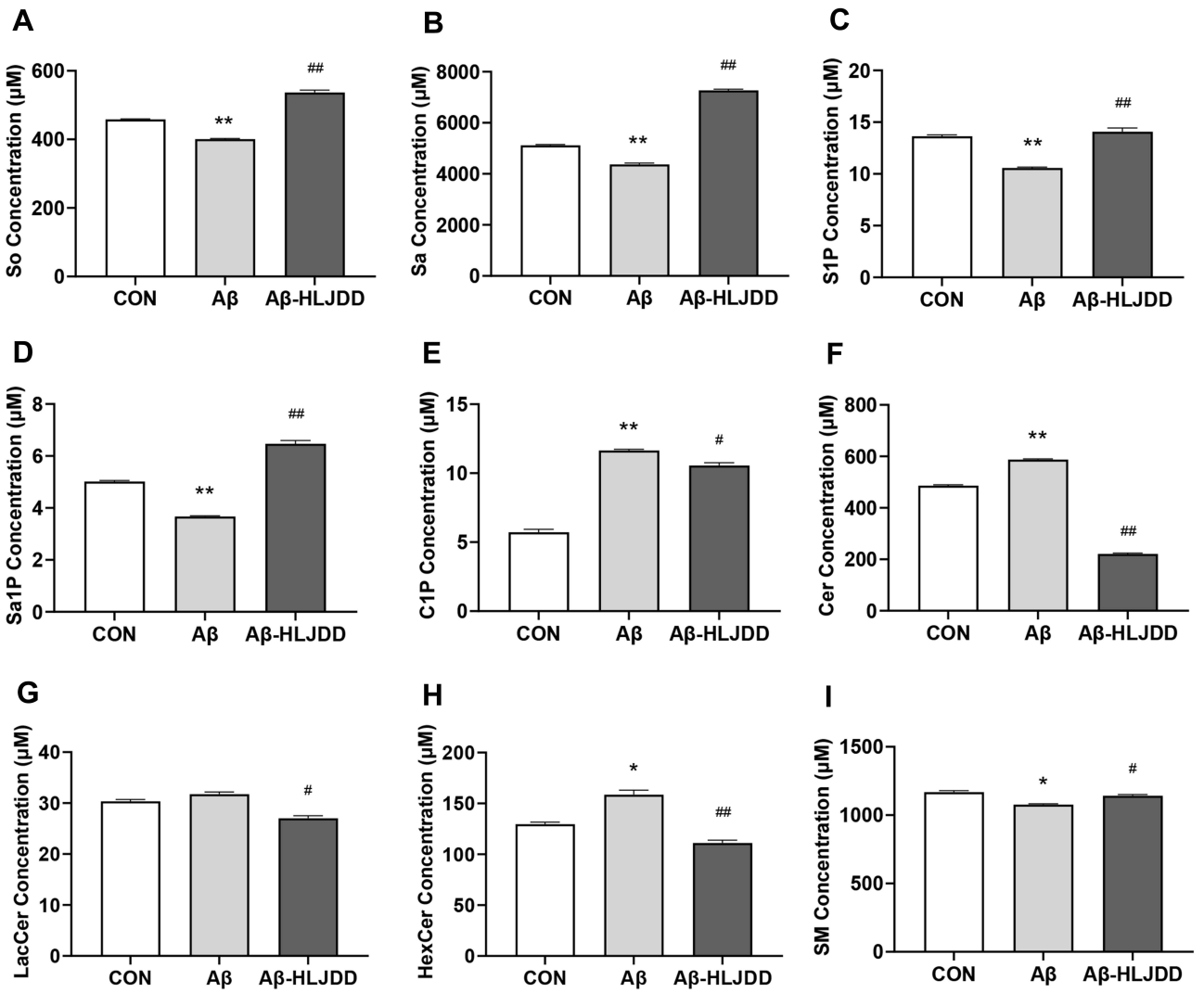

Figure 4 Sphingolipid metabolites secreted by Aβ-stimulated BV2 microglia with HLJDD. Total level of So (**A**), Sa (**B**), S1P (**C**), Sa1P (**D**), C1P (**E**), Cer (**F**), LacCer (**G**), HexCer (**H**), and SM (**I**) in BV2 microglia culture medium. Data were shown as the means±SD (n ≥ 6, CON vs Aβ, $^{*}p < 0.05$, $^{**}p < 0.01$; Aβ vs Aβ-HLJDD, $^{\#}p < 0.05$, $^{\#\#}p < 0.01$).

CSF containing HLJDD. Through this research, we tried to study the role of HLJDD in AD as it relates to lipid metabolism, especially sphingolipid metabolism.

To avoid the interference of complex components in the serum and to increase the relevancy of the research about the effectiveness of TCM,[37–39] medicated CSF was taken for in vitro studies. Nine active components of HLJDD, including berberine, berberrubine, palmatine, jatrorrhizine, baicalin, wogonin, oroxylin A, geniposide, and gardenin B were detected in CSF containing HLJDD, which proved that they could pass the blood-brain barrier to exert effects. The top three ingredients were geniposide, berberine and berberrubine.[28] A large number of researches have reported that geniposide may play a role in the treatment of AD by enhancing autophagy and lysosomal clearance of Aβ fibrils,[40] inhibiting nuclear factor kappa B,[41] enhancing cholinergic neurotransmission,[42] suppressing the mitochondrial oxidative damage and increasing the mitochondrial membrane potential and activity of cytochrome c oxidase.[43] Berberine could alleviate Aβ-induced mitochondrial dysfunction and synaptic loss,[44] target the hyper phosphorylation of tau and the autophagy clearance of tau,[45] and activate AMP-activated protein kinase. At present, studies on anti-AD of berberrubine are rare, but its derivatives displayed high antioxidant activity, and had the great ability to inhibit Aβ aggregation.[46] There was evidences that most of other ingredients may be candidate drugs for AD, such as palmatine,[36] jatrorrhizine,[36] baicalin,[47] wogonin,[48,49] and geniposide.[40] It is well known that TCM formula is a complex system, although these

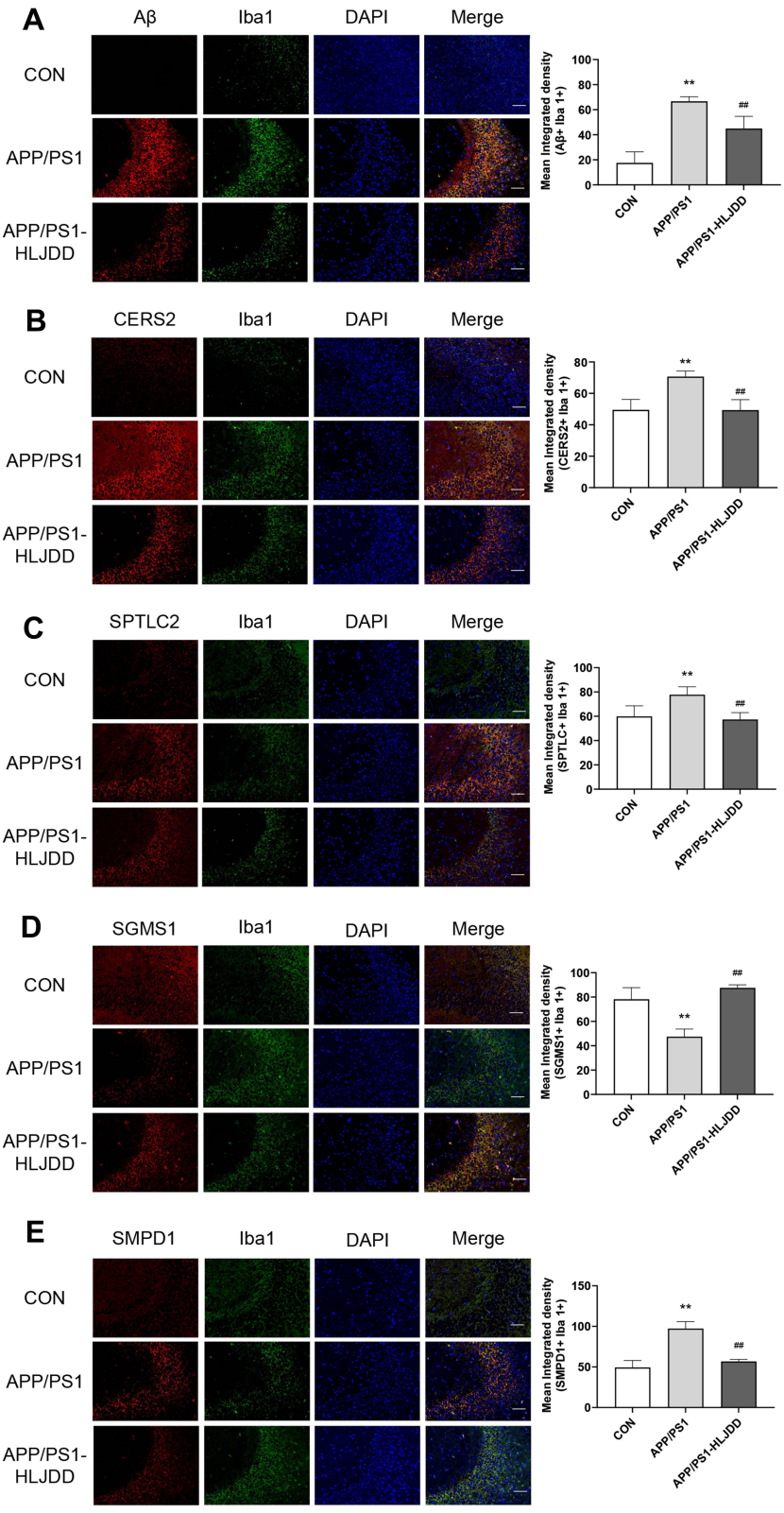

Figure 5 The levels of sphingolipid metabolizing enzymes in APP/PS1 mice. Representative immunofluorescence results of Aβ (**A**), CERS2 (**B**), SPTLC2 (**C**), SGMS1 (**D**), and SMPD1 (**E**) in microglia in hippocampal CA3 region; scale bar, 50 μm. Six random images per section and n=4 mice per group were analyzed. Data were shown as the means ±SD (CON vs APP/PS1, $^{**}p < 0.01$; APP/PS1 vs APP/PS1-HLJDD, $^{\#\#}p < 0.01$).

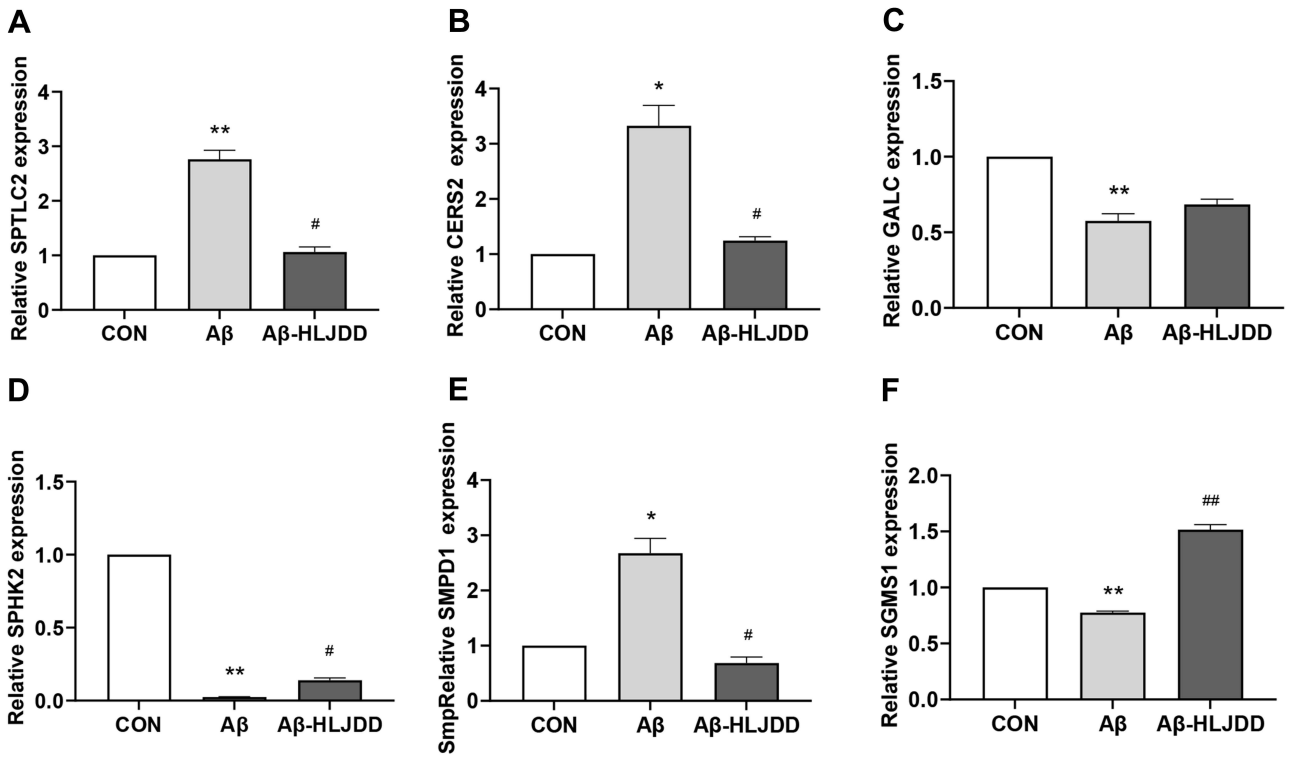

Figure 6 Transcription levels of sphingolipid metabolizing enzymes in BV2 microglia. mRNA levels of SPTLC2 (**A**), CERS2 (**B**), GALC (**C**), SPHK2 (**D**), SMPD1 (**E**), and SGMS1 (**F**). Data were shown as the means±SD (n ≥ 6, CON vs Aβ, $^{*}p < 0.05$, $^{**}p < 0.01$; Aβ vs Aβ-HLJDD, $^{\#}p < 0.05$, $^{\#\#}p < 0.01$).

components in CSF were low, combinations of them can make the prescriptions more suitable for clinical application through component-component synergic interactions that improve pharmacological activities.

Researches in the past decade have clearly indicated that sphingolipids are not only the structural components of the cell membrane but also act as signal molecules controlling a majority of cellular events, including signal transduction, cell growth, differentiation, and apoptosis.[50–52] Studies suggested that even minor changes in sphingolipid balance may play significant roles in the development of AD.[53]

It was found that with ageing, an increase in various stress factors and the deposition of Aβ, SMPD can hydrolyse SM to produce Cer, which in turn can not only stabilize the activity of APP lyase 1 and promote Aβ production but also induce apoptosis by the recombinant plasma membrane.[6,54] The increase level of Cer in AD brains has a toxic effect on neurons; additionally, it can promote the production of cytokines IL-2 and IL-6 and trigger neuro-inflammation.[55,56] According to our results, Cers had the most obvious changes, which could be one of the specific biomarkers against AD. Cers, the central molecules in the biosynthesis and catabolism of sphingolipids, are mainly derived from three pathways: the de novo synthesis pathway of serine and palmitoyl CoA, the cyclic pathway of reacylation of So and the biodegradation pathway of sphingolipids[57] (Figure 6). All sphingolipids are connected in the phospholipid bilayer by Cer. Analysis of epidemiological evidence of the role of Cer in AD revealed elevated levels of Cer in AD patients. Increased Cer levels prior to the clinical diagnostic stage of AD may be related to the etiopathophysiology of the disease.[58–60] Specifically, evidence regarding Cer C16:0 and Cer C24:1 is particularly strong.[61–65] SM may be another specific biomarker against AD. However, the changes in SMs are more complex, as the levels of different SMs species are inconsistent in different AD clinical studies.[61,66,67] Overall, SMs appears to have a trend toward lower levels associated with AD, although only a few studies have been published. Our results are consistent with the above clinical findings, which at least provide experimental support for identifying which Cer and/or SM species are associated with AD and can serve as biomarkers.

Besides Cer and SM, it was found that the contents of So and Sa were significantly reduced in the urine of AD patients.[4] As an intermediate product of sphingolipid metabolism, S1P can not only act as a cell signal molecule to

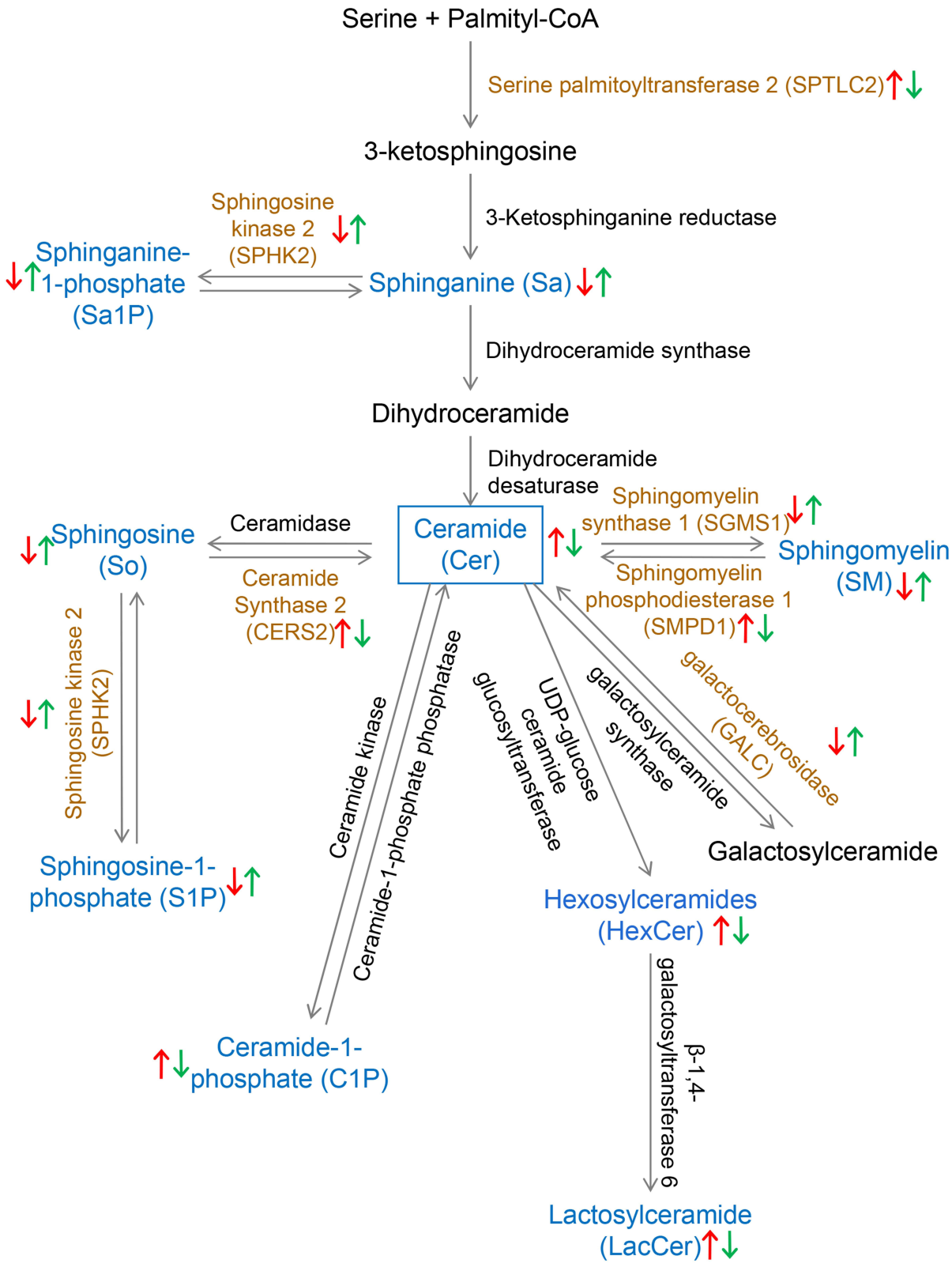

Figure 7 Diagram of the sphingolipid metabolism pathway in BV2 microglia. The red arrow indicates the sphingolipid components (blue) and sphingolipid metabolism-related enzymes (brown) that are upregulated or downregulated after $A\beta_{25-35}$ oligomer induction; the green arrow indicates the sphingolipid components (blue) and sphingolipid metabolism-related enzymes (brown) that are upregulated or downregulated after HLJDD treatment.

regulate cell proliferation, differentiation, adhesion and migration, but also act as a second messenger to regulate the concentration of intracellular Ca^{2+} and affect cell growth. A decrease in S1P was found in the brains of AD patients.[6,68]

Our results suggest that HLJDD has shown significant improvement in disordered sphingolipid metabolism, both in vivo and in vitro. In Japan, HLJDD has been used as a common prescription for the treatment of AD, and its effect on stroke sequelae and cerebrovascular dementia has been recognized.[69] Moreover, the addition of orengedoku-to (the same prescription of HLJDD in Japan) to yokukan-san (Kampo prescription) exerted the same efficacy as aripiprazole in controlling aggressiveness in an Alzheimer's-type dementia patient without any adverse effects.[21] Clinically, HLJDD could reduce the level of inflammatory factors in patients with AD, reduce the toxic and side effects caused by pitavastatin, improve the treatment efficiency and ensure medication safety.[70] Recently, HLJDD has achieved remarkable efficacy in the treatment of AD with the specific characteristics of anti-inflammation and oxidation resistance, preserving energy metabolism, reducing Aβ production, and improving memory in AD mice.[71–74] In summary, based on the current experimental results and existing clinical evidence, HLJDD is a Chinese herbal formula with good prospects for the treatment or adjuvant treatment of AD.

Of note, the levels of Cer and its derivatives were significantly changed in both APP/PS1 mice and $A\beta_{25\text{-}35}$-stimulated microglia, which provides partial support for further research on improving AD by regulating sphingolipids. More attention should be paid to the specific relationship between AD and key sphingolipids, which may help give better insights into the pathogenesis of AD and the potential mechanism of HLJDD treatment in AD.

Abbreviations

AD, Alzheimer's disease; Aβ, β-amyloid; BBR, blood brain barrier; Cer, ceramide; CERS2, ceramide synthase 2; CMC-Na, carboxymethyl cellulose sodium salt; C1P, ceramide-1-phosphate; CSF, cerebrospinal fluid; ESI, electrospray ion; GALC, galactosylceramidase; GalCer, galactosylceramide; GAPDH, glyceraldehyde-3-phosphate dehydrogenase; HexCer, hexosylceramide; HLJDD, Huanglian Jiedu decoction; Iba1, ionized calcium-binding adapter molecule 1; IL-1β, interleukin-1β; IOD, integral optical density; LacCer, lactosylceramide; OD, optical density; OPLS-DA, orthogonal projection to latent structures discriminant analysis; QC, quality control; qRT-PCR, Real-time quantitative reverse transcription-polymerase chain reaction; ROI, regions of interest; Sa, sphinganine; Sa1P, sphinganine-1-phosphate; SGMS1, sphingomyelin synthase 1; SM, sphingomyelin; SMPD1, sphingomyelin phosphodiesterase 1; So, sphingosine; S1P, sphingosine-1-phosphate; SPHK2, sphingosine kinase 2; SPTLC2, serine palmitoyltransferase 2; TCM, traditional Chinese medicine; WT, wild type.

Funding

This research was financially supported by the National Natural Science Foundation of China (Project Nos. 81573635 and 81873027), the Qing-Lan Project of Jiangsu Province, the Open Project Program of Jiangsu Key Laboratory for Pharmacology and Safety Evaluation of Chinese Materia Medica (No. JKLPSE201820), the Project Funded by the Priority Academic Program Development of Jiangsu Higher Education Institutions (PAPD), the Project of the Innovation Research Team of Nanjing University of Chinese Medicine, and the Project Funded by the Six Talent Project in Jiangsu Province.

Disclosure

The authors report no conflicts of interest for this work and declare that the research was conducted in the absence of any commercial or financial relationships that could be construed as a potential conflict of interest.

References

1. Selkoe DJ. Aging, amyloid, and Alzheimer's disease: a perspective in honor of Carl Cotman. *Neurochem Res*. 2003;28:1705–1713. doi:10.1023/a:1026065122854
2. Gu X, Zhou J, Zhou Y, et al. Huanglian Jiedu decoction remodels the periphery microenvironment to inhibit Alzheimer's disease progression based on the "brain-gut" axis through multiple integrated omics. *Alzheimers Res Ther*. 2021;13:44. doi:10.1186/s13195-021-00779-7
3. Vetrivel KS, Thinakaran G. Membrane rafts in Alzheimer's disease beta-amyloid production. *Biochim Biophys Acta*. 2010;1801:860–867. doi:10.1016/j.bbalip.2010.03.007

4. Li NJ, Li Y, Li Y. Detection of urine biomarkers in patients with Alzheimer's disease. *Chin Med Herald*. 2013;10:7–9. doi:10.3969/j.issn.1673-7210.2013.17.003
5. Wang Z. Study on the biomarkers regulation mechanism of Valeriana amurensis extractive on Aβ25-35 induced Alzheimer's disease mouse model. *J Tradit Chin Med*. 2017;32:5147–5150.
6. He X, Huang Y, Li B, Gong CX, Schuchman EH. Deregulation of sphingolipid metabolism in Alzheimer's disease. *Neurobiol Aging*. 2010;31:398–408. doi:10.1016/j.neurobiolaging.2008.05.010
7. Topisirovic I, Svitkin YV, Sonenberg N, Shatkin AJ. Cap and cap-binding proteins in the control of gene expression. *Wiley Interdiscip Rev RNA*. 2011;2:277–298. doi:10.1002/wrna.52
8. Kosicek M, Kirsch S, Bene R, et al. Nano-HPLC-MS analysis of phospholipids in cerebrospinal fluid of Alzheimer's disease patients–a pilot study. *Anal Bioanal Chem*. 2010;398:2929–2937. doi:10.1007/s00216-010-4273-8
9. Wood PL. Lipidomics of Alzheimer's disease: current status. *Alzheimers Res Ther*. 2012;4:5. doi:10.1186/alzrt103
10. Yuyama K, Sun H, Mitsutake S, Igarashi Y. Sphingolipid-modulated exosome secretion promotes clearance of amyloid-beta by microglia. *J Biol Chem*. 2012;287:10977–10989. doi:10.1074/jbc.M111.324616
11. Nayak D, Huo Y, Kwang WXT, et al. Sphingosine kinase 1 regulates the expression of proinflammatory cytokines and nitric oxide in activated microglia. *Neuroscience*. 2010;166:132–144. doi:10.1016/j.neuroscience.2009.12.020
12. Wang YY. Thinking about the difficulty of improving the curative effect of cerebrovascular disease. *Chin J Integr Trad West Med*. 1997;17:195–196.
13. Liu XH, Wang DD, Yu GR. Implication of the pathogenesis of "toxin impairing cerebral collaterals" in Alzheimer's disease. *J Henan Trad Chin Med*. 2017;37:90–92.
14. Shao W, Huang B, Pan XF, Zhang ZW, Chen GH. Clinical observation on senile dementia patients by Huperzine combined with Huanglianjiedu Soup. *Hubei J TCM*. 2012;34:11–12.
15. Liu N. Observe on the curative effect of Huanglian Jiedu decoction combined with Tianwang Buxin Dan in the treatment of heart and liver Yin deficiency type senile dementia. *Mod J Integr Trad Chin West Med*. 2016;25:1271–1273.
16. Chen GH, Shan P, Qiu X. The clinical study on Huanglianjiedu decoction on for patients with Senile Dementia, the type of hyperactivity of heart-fire and liver fire in TCM. *J Emerg TCM*. 2007;16:386–434.
17. Li H, Pan LM, Zhu HX. A review of pharmacodynamics of Huanglian Jiedu decoction on Alzheimer's disease. *J Trad Chin Med Liter*. 2010;28:45.
18. Zhang J, Zhang YL, Guo RJ, Chen ZG, Wang Y. From toxin damaging brain collaterals to toxin damaging collaterals. *Beijing J Trad Chin Med*. 2013;32:483–486.
19. Qi YY, Zhang QC, Zhu HX. Huang-Lian Jie-Du decoction: a review on phytochemical, pharmacological and pharmacokinetic investigations. *Chin Med*. 2019;14:57. doi:10.1186/s13020-019-0277-2
20. Fang H, Wang Y, Yang T, et al. Bioinformatics analysis for the antirheumatic effects of huang-lian-jie-du-tang from a network perspective. *Evid Based Complement Alternat Med*. 2013;2013:245357. doi:10.1155/2013/245357
21. Okamoto H, Chino A, Hirasaki Y, et al. Orengedoku-to augmentation in cases showing partial response to yokukan-san treatment: a case report and literature review of the evidence for use of these Kampo herbal formulae. *Neuropsychiatr Dis Treat*. 2013;9:151–155. doi:10.2147/NDT.S38318
22. Xu J, Murakami Y, Matsumoto K, et al. Protective effect of Oren-gedoku-to (Huang-Lian-Jie-Du-Tang) against impairment of learning and memory induced by transient cerebral ischemia in mice. *J Ethnopharmacol*. 2000;73:405–413. doi:10.1016/s0378-8741(00)00303-2
23. Kondo Y, Kondo F, Asanuma M, Tanaka K, Ogawa N. Protective effect of oren-gedoku-to against induction of neuronal death by transient cerebral ischemia in the C57BL/6 mouse. *Neurochem Res*. 2000;25:205–209. doi:10.1023/a:1007515318434
24. Gu XR, Fang SY, Ren W, et al. [Pharmacodynamics of Huanglian Jiedu decoction in Alzheimer's disease (AD) model rats and effect on improvement of inflammation microenvironment in brain]. *Chin J Chin Mate Med*. 2018;43:3006–3011. Chinese. doi:10.19540/j.cnki.cjcmm.2018.0092
25. Sun LM, Zhu B-J, Cao H-T, et al. Explore the effects of Huang-Lian-Jie-Du-Tang on Alzheimer's disease by UPLC-QTOF/MS-based plasma metabolomics study. *J Pharm Biomed Anal*. 2018;151:75–83. doi:10.1016/j.jpba.2017.12.053
26. Zeng MF, Pan LM, Zhu HX, Zhang QC, Guo LW. Pharmacokinetics of geniposide in Huanglian Jiedu Decoction in normal and cerebral ischemia rats. *Chin Tradit Herb Drugs*. 2010;41:617–620.
27. Wang JR, Zhang H, Yau LF, et al. Improved sphingolipidomic approach based on ultra-high performance liquid chromatography and multiple mass spectrometries with application to cellular neurotoxicity. *Anal Chem*. 2014;86:5688–5696. doi:10.1021/ac5009964
28. Heng X. Distribution characteristics of nine main components of Huanglian Jiedu Decoction in rat brain. *Chin Tradit Herb Drugs*. 2020;51:3922–3929.
29. Hao LN, Zhang QZ, Yu TG, Cheng YN, Ji SL. Antagonistic effects of ultra-low-molecular-weight heparin on Aβ25-35-induced apoptosis in cultured rat cortical neurons. *Brain Res*. 2011;1368:1–10. doi:10.1016/j.brainres.2010.10.064
30. Livak KJ, Schmittgen TD. Analysis of relative gene expression data using real-time quantitative PCR and the 2(-Delta Delta C(T)) method. *Methods*. 2001;25:402–408. doi:10.1006/meth.2001.1262
31. Sullards MC, Liu Y, Chen Y, Merrill AH. Analysis of mammalian sphingolipids by liquid chromatography tandem mass spectrometry (LC-MS/MS) and tissue imaging mass spectrometry (TIMS). *Biochim Biophys Acta*. 2011;1811:838–853. doi:10.1016/j.bbalip.2011.06.027
32. Xing PP. *Effect of Sea Cucumber Cerebrosides on Related Sphingolipids in Brain Tissue of Alzheimer's Disease Model Mice*. Ocean University of China; 2014.
33. Zhang F, Zhong R, Li S, et al. Acute hypoxia induced an imbalanced M1/M2 activation of microglia through NF-kappaB signaling in Alzheimer's disease mice and wild-type littermates. *Front Aging Neurosci*. 2017;9:282. doi:10.3389/fnagi.2017.00282
34. Wang F, Chen XG. The advance of Huanglian Jiedu Decoction in prevention and cure of Senile Dementia. *J Liaoning Univ Tradit Chin Med*. 2015;17:86–89.
35. Lu J, Wang JS, Kong LY. Anti-inflammatory effects of Huang-Lian-Jie-Du decoction, its two fractions and four typical compounds. *J Ethnopharmacol*. 2011;134:911–918. doi:10.1016/j.jep.2011.01.049
36. Yu CJ, Zheng MF, Kuang CX, Huang WD, Yang Q. Oren-gedoku-to and its constituents with therapeutic potential in Alzheimer's disease inhibit indoleamine 2, 3-dioxygenase activity in vitro. *J Alzheimers Dis*. 2010;22:257–266. doi:10.3233/JAD-2010-100684

37. Hu HY, Xi DZ, Lei L, Chen X, Wang WH. Protective mechanism of cerebrospinal fluid containing Qingxin Kaiqiao recipe on PC12 cell injury induced by glutamate. *Chin J Chin Mate Med*. 2013;38:1997–2000. doi:10.4268/cjcmm20131230
38. Li FD, Wang YH, Zhang C, Wen W, Huang SM. The growth-promoting effect of Kaixin powder-containing cerebrospinal fluid on cultured PC12 cells without serum. *J Chin Med Pharmacol*. 2012;40:12–14. doi:10.3969/j.issn.1002-2392.2012.06.005
39. Qin XD, Liu Y, Zhang YL, Wang S, Zhu JQ, Kang LY. Effect of Qingnao Yizhi decoction on synaptic remodeling related indexes. *Chin J Exp Tradit Med Form*. 2013;019:174–177. doi:10.11653/syfj2013100174
40. Zhang Z, Wang X, Zhang D, Liu Y, Li L. Geniposide-mediated protection against amyloid deposition and behavioral impairment correlates with downregulation of mTOR signaling and enhanced autophagy in a mouse model of Alzheimer's disease. *Aging*. 2019;11:536–548. doi:10.18632/aging.101759
41. Seo EJ, Fischer N, Efferth T. Phytochemicals as inhibitors of NF-kappaB for treatment of Alzheimer's disease. *Pharmacol Res*. 2018;129:262–273. doi:10.1016/j.phrs.2017.11.030
42. Zhao C, Zhang H, Li H, et al. Geniposide ameliorates cognitive deficits by attenuating the cholinergic defect and amyloidosis in middle-aged Alzheimer model mice. *Neuropharmacology*. 2017;116:18–29. doi:10.1016/j.neuropharm.2016.12.002
43. Lv C, Liu X, Liu H, Chen T, Zhang W. Geniposide attenuates mitochondrial dysfunction and memory deficits in APP/PS1 transgenic mice. *Curr Alzheimer Res*. 2014;11:580–587. doi:10.2174/1567205011666140618095925
44. Zhao C, Su P, Lv C, et al. Berberine alleviates amyloid β-induced mitochondrial dysfunction and synaptic loss. *Oxid Med Cell Longev*. 2019;2019:7593608. doi:10.1155/2019/7593608
45. Chen Y, Chen Y, Liang Y, et al. Berberine mitigates cognitive decline in an Alzheimer's disease mouse model by targeting both tau hyperphosphorylation and autophagic clearance. *Biomed Pharmacother*. 2020;121:109670. doi:10.1016/j.biopha.2019.109670
46. Jiang H, Wang X, Huang L, et al. Benzenediol-berberine hybrids: multifunctional agents for Alzheimer's disease. *Bioorg Med Chem*. 2011;19:7228–7235. doi:10.1016/j.bmc.2011.09.040
47. Zhao J, Lu S, Yu H, Duan S, Zhao J. Baicalin and ginsenoside Rb1 promote the proliferation and differentiation of neural stem cells in Alzheimer's disease model rats. *Brain Res*. 2018;1678:187–194. doi:10.1016/j.brainres.2017.10.003
48. Huang DS, Yu YC, Wu CH, Lin JY. Protective effects of Wogonin against Alzheimer's disease by inhibition of amyloidogenic pathway. *Evid Based Complement Alternat Med*. 2017;2017:3545169. doi:10.1155/2017/3545169
49. Zhu Y, Wang J. Wogonin increases beta-amyloid clearance and inhibits tau phosphorylation via inhibition of mammalian target of rapamycin: potential drug to treat Alzheimer's disease. *Neurol Sci*. 2015;36:1181–1188. doi:10.1007/s10072-015-2070-z
50. Hannun YA, Obeid LM. The Ceramide-centric universe of lipid-mediated cell regulation: stress encounters of the lipid kind. *J Biol Chem*. 2002;277:25847–25850. doi:10.1074/jbc.R200008200
51. Ohanian J, Ohanian V. Sphingolipids in mammalian cell signalling. *Cell Mol Life Sci*. 2001;58:2053–2068. doi:10.1007/PL00000836
52. Holthuis JC, Pomorski T, Raggers RJ, Sprong H, Van Meer G. The organizing potential of sphingolipids in intracellular membrane transport. *Physiol Rev*. 2001;81:1689–1723. doi:10.1152/physrev.2001.81.4.1689
53. Mielke MM, Lyketsos CG. Alterations of the sphingolipid pathway in Alzheimer's disease: new biomarkers and treatment targets? *Neuromolecular Med*. 2010;12:331–340. doi:10.1007/s12017-010-8121-y
54. Puglielli L, Ellis BC, Saunders AJ, Kovacs DM. Ceramide stabilizes beta-site amyloid precursor protein-cleaving enzyme 1 and promotes amyloid beta-peptide biogenesis. *J Biol Chem*. 2003;278:19777–19783. doi:10.1074/jbc.M300466200
55. Ballou LR, Laulederkind SJ, Rosloniec EF, Raghow R. Ceramide signalling and the immune response. *Biochim Biophys Acta*. 1996;1301:273–287. doi:10.1016/0005-2760(96)00004-5
56. Cutler RG, Kelly J, Storie K, et al. Involvement of oxidative stress-induced abnormalities in ceramide and cholesterol metabolism in brain aging and Alzheimer's disease. *Proc Natl Acad Sci U S A*. 2004;101:2070–2075. doi:10.1073/pnas.0305799101
57. Pralhada Rao R, Vaidyanathan N, Rengasamy M, et al. Sphingolipid metabolic pathway: an overview of major roles played in human diseases. *J Lipids*. 2013;2013:178910. doi:10.1155/2013/178910
58. Satoi H, Tomimoto H, Ohtani R, et al. Astroglial expression of ceramide in Alzheimer's disease brains: a role during neuronal apoptosis. *Neuroscience*. 2005;130:657–666. doi:10.1016/j.neuroscience.2004.08.056
59. Han X, McKeel DW, Kelley J, Morris JC, Morris JC. Substantial sulfatide deficiency and ceramide elevation in very early Alzheimer's disease: potential role in disease pathogenesis. *J Neurochem*. 2002;82:809–818. doi:10.1046/j.1471-4159.2002.00997.x
60. Katsel P, Li C, Haroutunian V. Gene expression alterations in the sphingolipid metabolism pathways during progression of dementia and Alzheimer's disease: a shift toward ceramide accumulation at the earliest recognizable stages of Alzheimer's disease? *Neurochem Res*. 2007;32:845–856. doi:10.1007/s11064-007-9297-x
61. Huynh K, Lim WLF, Giles C, et al. Concordant peripheral lipidome signatures in two large clinical studies of Alzheimer's disease. *Nat Commun*. 2020;11:5698. doi:10.1038/s41467-020-19473-7
62. Kim M, Nevado-Holgado A, Whiley L, et al. Association between plasma ceramides and phosphatidylcholines and hippocampal brain volume in late onset Alzheimer's disease. *J Alzheimers Dis*. 2017;60:809–817. doi:10.3233/JAD-160645
63. Savica R, Murray ME, Persson X-M, et al. Plasma sphingolipid changes with autopsy-confirmed Lewy Body or Alzheimer's pathology. *Alzheimers Dement*. 2016;3:43–50. doi:10.1016/j.dadm.2016.02.005
64. Xing Y, Tang Y, Zhao L, et al. Plasma ceramides and neuropsychiatric symptoms of Alzheimer's disease. *J Alzheimers Dis*. 2016;52:1029–1035. doi:10.3233/JAD-151158
65. Gonzalez-Dominguez R, Garcia-Barrera T, Gomez-Ariza JL. Application of a novel metabolomic approach based on atmospheric pressure photoionization mass spectrometry using flow injection analysis for the study of Alzheimer's disease. *Talanta*. 2015;131:480–489. doi:10.1016/j.talanta.2014.07.075
66. Armirotti A, Basit A, Realini N, et al. Sample preparation and orthogonal chromatography for broad polarity range plasma metabolomics: application to human subjects with neurodegenerative dementia. *Anal Biochem*. 2014;455:48–54. doi:10.1016/j.ab.2014.03.019
67. Han X, Rozen S, Boyle SH, et al. Metabolomics in early Alzheimer's disease: identification of altered plasma sphingolipidome using shotgun lipidomics. *PLoS One*. 2011;6:e21643. doi:10.1371/journal.pone.0021643
68. Couttas TA, Kain N, Daniels B, et al. Loss of the neuroprotective factor Sphingosine 1-phosphate early in Alzheimer's disease pathogenesis. *Acta Neuropathol Commun*. 2014;2:9. doi:10.1186/2051-5960-2-9

69. Chen ZY, Yue RS, Zhang XK. Summary of research on traditional Chinese medicine for cerebrovascular dementia. *J Pract Tradit Chin Intern Med*. 2005;19:494–496.
70. Chen HL, Guan F. Mechanism of Huanglian Jiedu Decoction to promote pitavastatin treatment of Alzheimer's disease. *J Hainan Med Univ*. 2016;22:2283–2286. doi:10.13210/j.cnki.jhmu.20160620.001
71. Qiu X, Chen GH, Wang T. [Effects of huanglian jiedu decoction on free radicals metabolism and pathomorphism of the hippocampus in App/PS1 double transgenic mice]. *Chin J Integr Trad West Med*. 2011;31:1379–1382. Chinese. doi:10.1097/MOP.0b013e328341d1da
72. Wang PR, Wang J-S, Zhang C, et al. Huang-Lian-Jie-Du-Decotion induced protective autophagy against the injury of cerebral ischemia/reperfusion via MAPK-mTOR signaling pathway. *J Ethnopharmacol*. 2013;149:270–280. doi:10.1016/j.jep.2013.06.035
73. Wang S, Jiang N, Zhou WX, Zhang YY. [Effect of Huanglian Jiedutang on expression of hippocampus proteomics in senescence accelerated mouse]. *Chin J Chin Mate Med*. 2007;32:2289–2294. Chinese.
74. Nie X, Deng R, Xiang L, Jiang P, Xue Q. Reno-protective effect and mechanism study of Huang Lian Jie Du Decoction on lupus nephritis MRL/lpr mice. *BMC Complement Altern Med*. 2016;16:448. doi:10.1186/s12906-016-1433-1